OENO One
VINE AND WINE OPEN ACCESS JOURNAL
By IVES International Viticulture & Enology Society

2nd ClimWine Symposium
terclim
July 3 – 8, 2022 | Bordeaux, France
XIVth International Terroir Congress

DOI:10.20870/oeno-one.2022.56.2.5435

OPEN ACCESS

ORIGINAL RESEARCH ARTICLE

Variety-specific response of bulk stomatal conductance of grapevine canopies to changes in net radiation, atmospheric demand, and drought stress

Mark Gowdy[1], Bruno Suter[1], Philippe Pieri[1], Elisa Marguerit[1], Agnès Destrac Irvine[1], Gregory A. Gambetta[1] and Cornelis van Leeuwen[1*]

[1] EGFV, Univ. Bordeaux, Bordeaux Sciences Agro, INRAE, ISVV, F-33882 Villenave d'Ornon, France

This article is published in cooperation with Terclim 2022 (XIVth International Terroir Congress and 2nd ClimWine Symposium), 3-8 July 2022, Bordeaux, France.

*correspondence:
vanleeuwen@agro-bordeaux.fr

Associate editor:
Hans Schultz

Received:
28 February 2022

Accepted:
14 April 2022

Published:
24 June 2022

ABSTRACT

In wine growing regions around the world, climate change has the potential to affect vine transpiration and overall vineyard water use due to related changes in daily atmospheric conditions and soil water deficits. Grapevines control their transpiration in response to such changes by regulating conductance of water through the soil-plant-atmosphere continuum. The response of bulk stomatal conductance, the vine canopy equivalent of stomatal conductance, to such changes were studied on Cabernet-Sauvignon, Merlot, Tempranillo, Ugni blanc, and Semillon vines in a non-irrigated vineyard in Bordeaux France. Whole-vine sap flow, temperature and humidity in the vine canopy, and net radiation absorbed by the vine canopy were measured on 15-minute intervals from early July through mid-September 2020, together with periodic measurements of leaf area, canopy porosity, and predawn leaf water potential. From these data, bulk stomatal conductance was calculated on 15-minute intervals, and multiple linear regression analysis was performed to identify key variables and their relative effect on conductance. For the regression analysis, attention was focused on addressing non-linearity and collinearity in the explanatory variables and developing a model that was readily interpretable.

Variability of vapour pressure deficit in the vine canopy over the day and predawn water potential over the season explained much of the variability in bulk stomatal conductance overall, with relative differences between varieties appearing to be driven in large part by differences in conductance response to predawn water potential between the varieties. Transpiration simulations based on the regression equations found similar differences between varieties in terms of daily and seasonal transpiration. These simulations also compared well with those from an accepted vineyard water balance model, although there appeared to be differences between the two approaches in the rate at which conductance, and hence transpiration is reduced as a function of decreasing soil water content (i.e., increasing water deficit stress). By better characterizing the response of bulk stomatal conductance, the dynamics of vine transpiration can be better parameterized in vineyard water use modeling of current and future climate scenarios.

KEYWORDS: grapevine, climate change, drought stress, vineyard water use models, *Vitis vinifera*, cultivar

INTRODUCTION

Grapevines regulate their water use in response to changing atmospheric demand and drought stress by regulating the conductance of water through the soil-plant-atmosphere continuum (McElrone *et al.*, 2013). This conductance is regulated by various physiological mechanisms such as control of stomatal aperture and hydraulic conductivity of the vasculature (Lovisolo *et al.*, 2010). The resistance to water vapour diffusion through open stomata is much greater than the resistance of water through the vasculature, with that through the stomata becoming the controlling factor in overall transpiration (Sack and Holbrook, 2006; Krounbi and Lazarovitch, 2011). Stomatal regulation of conductance varies diurnally (Bai *et al.*, 2015; Lu *et al.*, 2003; Zhang *et al.*, 2012), across the season (Herrera *et al.*, 2021), and with differences in response to changing environmental variables observed between varieties (Costa *et al.*, 2012; Prieto *et al.*, 2010).

Plant species that readily close their stomata to reduce transpiration and maintain constant leaf water potential when faced with increasing vapour pressure deficit, and/or decreasing soil water status are classified as *isohydric*, while those that keep their stomata open and allow for more negative leaf water potential are classified as *anisohydric* (Tardieu and Simonneau, 1998). This stomatal regulation, however, does not always fit neatly into these categories (Martínez-Vilalta *et al.*, 2014), with some species demonstrating responses that vary with water stress (Levin *et al.*, 2020), or a hybrid response such as *isohydrodynamic*, whereby stomata are regulated to maintain a roughly constant difference between leaf and soil water potential (Franks *et al.*, 2007; Domec and Johnson, 2012; Zhang *et al.*, 2012; Charrier *et al.,* 2018). Within the species *Vitis vinifera*, different varieties demonstrate a range of response dynamics, which are difficult to categorize, or they display inconsistent dynamics across numerous different studies (Chaves *et al.*, 2010; Lavoie-Lamoureux *et al.*, 2017). For example, Syrah has often been found in studies to demonstrate anisohydric response (Prieto *et al.*, 2010; Schultz, 2003), but in others has demonstrated near-isohydric response for this variety (Pou *et al.*, 2012), although such differences could be attributable to soil and climate differences (Hochberg *et al*., 2018).

The ability of the soil to deliver water through its pore spaces to the roots is also a key component in the soil-plant-atmosphere continuum. Depending on the texture of the soil, water potential decreases as the soil water content decreases, particularly once the fraction of transpirable soil water drops below about 0.4 (Schultz, 1996; Lebon *et al.*, 2003) as experienced during drought conditions. This leads to a corresponding reduction in the hydraulic conductivity within the soil matrix supplying water to the roots (Krounbi and Lazarovitch, 2011; Tramontini *et al.*, 2012) and therefore the overall conductance across the soil-plant-atmosphere continuum, and hence stomatal conductance.

Crop evapotranspiration (ET_c) is often modeled using the FAO 56 approach of applying seasonally variable crop coefficients (K_c) to estimates of reference crop evapotranspiration (ET_o), which are calculated using the Penman Monteith (PM) equation based on an assumption of well-watered conditions and an associated fixed crop canopy conductance (Allen *et al.*, 1998). To account for drought stress this approach then applies a stress coefficient (K_s) to ET_c to calculate adjusted crop evapotranspiration ($ET_{c\,adj}$). K_s is assumed to be 1.0 (i.e., no water stress) until the modeled balance of available soil water decreases below a threshold value, below which the Ks decreases linearly to zero where the soil water content reaches the wilting point. A vineyard water balance model adapted from this FAO approach was developed by Lebon *et al.* (2003), although it is not parameterized to distinguish differences in transpiration between varieties.

Being able to characterize variety-specific changes in conductance in response to changing atmospheric conditions and drought would help improve modeling of the vine canopy transpiration component in vineyard water balance models, particularly for evaluating different adaptation strategies under future climate change scenarios. Therefore, the main goal of this study is to quantify and differentiate the response of bulk stomatal conductance (g_{bs}) of different grapevine varieties to changes in key environmental variables potentially affected by climate change, and to simulate transpiration using these relationships for comparison against an existing vineyard water balance model. As described by Gowdy *et al.* (2022), g_{bs} can be calculated in vineyards with open canopies based on an inverted Penman-Monteith type transpiration equation and the assumptions of the two-source energy flux approach developed by Shuttleworth and Wallace (1985). The total conductance of the vine canopy (g_{bs}) is effectively the stomatal conductance of every leaf in the canopy acting together in a parallel circuit, which conceptually is the sum of the stomatal conductance of all those leaves (Kelliher *et al.*, 1995).

The diffusion of water vapour through stomata is affected by: i) solar radiation, which provides energy for evaporation and diffusion; ii) vapour pressure deficit, which is the driving force for diffusion; and iii) the effects of boundary layer resistance to diffusion at the leaf surface (Keller, 2015). The stomatal openings themselves can also be affect by changes in light levels (Shimazaki *et al.*, 2007) and vapour pressure deficit (Oren *et al.*, 1999). By analogy at the vine canopy scale, the amount of net radiation absorbed by the vine canopy (R_c) provides the energy for canopy transpiration (Monteith and Unsworth, 2013) and can be affected by changes in cloud cover associated with climate change (Mendoza *et al.*, 2021) and global dimming/brightening associated with human-induced pollution and its interaction with the climate (Wild, 2009). Canopy dimensions are also an important factor in determining R_c (Riou *et al.*, 1989; Pieri, 2010) and can be modified by growers as an adaptation to climate change (van Leeuwen *et al.*, 2019a). Similarly, vapour pressure deficit in the canopy (D_c) may be affected by climate change related impacts on air and canopy temperatures, and the tendency towards lower relative humidity in near-surface air over land as observed in

the last 20 years in the mid-latitudes and Mediterranean (Willett *et al.*, 2014). Another variable for consideration is the leaf area index (*LAI*), which in turn affects bulk boundary layer resistance (Shuttleworth and Wallace, 1985; Lhomme *et al.*, 2012). *LAI* can be affected by vine vigour, which can depend on the variety, the rootstock and the available resources, such as water and nutrients (Smart and Robinson, 1991). Then, later in the season it can be affected by leaf drop. Grapevines are known to drop leaves in response to increasingly intense drought conditions as a way of controlling their transpiration (Zufferey *et al.*, 2011).

Additionally, vine water deficit stress can have an important effect on vine transpiration and conductance. Physiological vine responses, such as changes in photosynthesis, stomatal closure, and shoot growth characteristics in response to water deficit stress, are often correlated well with water potential (Lebon *et al.*, 2003; Pellegrino *et al.*, 2006). Measurement of predawn leaf water potential (Ψ_{PD}) is an accepted plant-based measurement of plant water status (Sperry *et al.*, 1996), which gives the water potential of the plant at the end of the night when the stomata are closed and the plant is in equilibrium with the root zone water potential (Choné *et al.*, 2001). Climate change has the potential to affect vine water stress if there are changes in precipitation and/or vineyard evapotranspiration. As an adaptation, the planting density of new vineyards can be decreased, or irrigation can be used (van Leeuwen *et al.*, 2019a; van Leeuwen *et al.*, 2019b).

In this paper, a multiple linear regression approach was used in an iterative fashion to develop an explanatory statistical model of calculated g_{bs} as the response variable against: i) net radiation absorbed by the vine canopy; ii) vapour pressure deficit in the vine canopy; and iii) predawn leaf water potential as the three predictor variables. The emphasis is on developing a model that is readily interpretable for the purpose of characterizing the dynamics of this response.

MATERIALS AND EQUIPMENT

The measurements for this study were taken on 10 individual grapevines in a vineyard, two each of *Vitis vinifera* L., cv. Cabernet-Sauvignon, Merlot, Tempranillo, Semillon, and Ugni blanc. Measurements of sap flow, temperature and humidity, and solar radiation were taken or interpolated to 15-minute intervals from 30 June through 15 September 2020 and canopy characteristics were measured periodically through the season.

1. Vineyard and canopy characteristics

The study was performed in a 0.6-hectare common garden experimental vineyard in Bordeaux, France (44° 47' 0" N, 0° 34' 39" W) with 52 varieties planted in a randomized block design, in which the varieties were planted in 5 replicate blocks of 10 vines each. All measured vines were located in different blocks of the vineyard, with the exception of the two Merlot vines, which were in two different rows within the same block. The vines are trained on a vertical shoot positioning trellis system with double Guyot pruning.

The top and bottom of the vine canopy are 1.5 m and 0.5 m above the ground respectively and 0.4 m wide, with canopy dimensions maintained by hedging twice during the growing season. Vine rows are orientated north-south with 1.8 m row spacing and 1.0 m vine spacing. There is a mowed cover crop in between each vine row with mechanical tillage under the vine row. The vines were planted on SO4 rootstock and the soils are sandy-clay-gravel typical for the Pessac-Léognan wine appellation (Destrac-Irvine and van Leeuwen, 2017). From 1991 through 2020 average annual total rainfall and reference evapotranspiration were 902 mm and 929 mm respectively with annual solar radiation of 4790 MJ m^{-2} and average maximum daily temperature from May through September of 25.5 C°.

Leaf area was measured three times during the season in the first halves of July, August and September respectively. Leaf area was determined on each vine by first measuring the length and width of all individual leaves on one primary shoot and all its secondary shoots, which averaged just over 100 leaves on each vine on each measurement date. Those dimensions were well correlated with individual leaf area as measured by a leaf area meter (Model LI-3100 LICOR Inc., Lincoln, NE, USA) before field measurements began. An average size of leaves on primary and secondary shoots were then calculated and applied to a count of all the leaves on the remaining primary and secondary shoots on each vine. Leaf area index (*LAI*, m^2 m^{-2}) is calculated as the total leaf area (m^2) for a vine divided by the area of vineyard ground attributable to each vine (i.e., row spacing x vine spacing). The porosity of each vine canopy was measured in the vineyard using a camera phone application (CANAPEO, Oklahoma State University Department of Plant and Soil Sciences, Stillwater, OK, USA) on the same dates as leaf area measurement with any missing measurements being filled in using a regression between measured leaf area and porosity.

2. Field measurements

Transpiration flux (E_c) was measured by heat balance sap flow sensors (Model SGEX, Dynamax Inc., Houston, TX, USA) that were installed on vine canes at a location where the flow of at least 30 % of the whole vine would be measured (based on the relative number of shoots downstream of the sensor). Sap flow (g s^{-1}) was calculated from sensor signals collected by a datalogger (Model SapIP, Dynamax Inc., Houston, TX, USA) and then scaled up for the whole vine based on the ratio of leaf area of the whole vine over the leaf area of shoots downstream the sap flow sensor. Sap flow (g s^{-1}) was then divided by the area of vineyard ground attributable to each vine (i.e., row spacing x vine spacing) to give canopy transpiration flux, E_c (g s^{-1} m^{-2}).

Vapour pressure deficit (D_c) was measured in the vine canopy at 1.15 m above the ground. This height was estimated to be that above which heat and vapour flux from both the vine canopy and ground surrounding the vine rows is well mixed (Shuttleworth and Wallace, 1985; Gowdy *et al.*, 2022). The mean canopy height was estimated using empirical relationships for vineyards based primarily on canopy height

(Chahine *et al.*, 2014). The saturation vapour pressure, e_{sc} (Pa) was calculated by Teten's equation using measured temperature T_c (C°) with the partial vapour pressure, e_c (Pa) calculated from e_{sc} using measured relative humidity. Temperature and humidity were measured using TinyTag Plus 2 probe/data loggers (Model TGP-4505 by Gemini Data Loggers, Chichester, West Sussex, England) with the temperature/relative humidity probes installed inside solar radiation shields (Model RS3 by Prosensor, Amanvillers, France) and hung from a trellis wire in the vine canopy at the mean canopy height.

Global (shortwave) radiation flux was measured at a weather station next to the vineyard using a horizontally mounted pyranometer (Model No. CMP6 by Kipp & Zonen, Delft - The Netherlands) on one-hour intervals, and then linearly interpolated to 15-minute intervals.

Measurements of Ψ_{PD} were taken on each vine in the study at six times during the season, roughly 10-14 days apart depending on weather, from early July through early September 2020. Sampling and measurement were done early enough to ensure all measurements were completed no later than 30 minutes prior to sunrise. Measurements were taken on one leaf per vine by the method of Scholander *et al.* (1965) using a pressure chamber with digital manometer (DG MECA, 33175 Gradignan, France).

METHODS

A multiple linear regression analysis was performed in an iterative fashion by: i) applying data filters and calculating bulk stomatal conductance; ii) making necessary data transformations; iii) selecting predictor variables to include in the final regression model; and iv) verifying that ordinary least squared assumptions are properly met in the final regression model. The intent of the above is to obtain a readily interpretable model with the best possible fit. While non-linear, or non-parametric regression analysis might provide a better fit with lower residuals, the coefficients from such models become less readily interpretable (Shmueli, 2010).

1. Data compilation and filtering

A database of R_c and D_c was compiled from measurements and estimates on 15-minute intervals from 30 June through 15 September 2020. Missing data were replaced by linear interpolation if there were no more than four missing 15-minute measurements between available data points, otherwise gaps in the data were maintained. Measurements of Ψ_{PD} and *LAI* were also included, but as they were obtained only periodically during the season, those data were interpolated to a daily time step using a local weighted regression (LOESS) curve between measurements. Over the study period there was only one significant rain event of 36 mm on 11 through 13 August 2020, with Ψ_{PD} taken just 4 days before and 7 days afterwards. During the remainder of the study period, no other daily rainfall total exceeded more than a few millimeters, which is well below an amount that would affect predawn water potential.

The equation for calculating g_{bs} (as described in the next section) was observed to give unrealistically high and erratic results when input values of R_c, D_c, or E_c were low, particularly in the early morning and evening. These low values also introduced irregularities in the residual plots for regressions that included them. The data, therefore, were filtered on a trial-and-error basis to eliminate these problems. Previous studies of conductance in vineyards took a similar approach of filtering low net radiation data to address such issues (Lu *et al.*, 2003; Zhang *et al.*, 2012).

The selected filters were applied separately to the data from individual vines when R_c < 90 W m^{-2} or D_c < 900 Pa or if E_c was less than the 30th percentile of all values for a given vine. The latter filter was applied on a percentile basis due to the differing ranges of E_c observed across the different vines measured. Otherwise, fixed filter thresholds might disproportionally remove more data from vines with generally lower E_c than other vines. The E_c data in general was strongly skewed towards lower values, so application of the filters removed data records at times when E_c was very low, resulting in only a 9 to 14 percent reduction, depending on the vine, in measured transpiration over the season. This reduction ranged slightly higher from 9 to 18 percent for transpiration during times when drought stress, as measured by predawn water potential was less than - 4.0 bars. The loss of these values was not considered significant for the purpose of regression analysis aimed at defining relationships at higher transpiration rates when the majority of vine water use actually takes place.

After the data from each vine was filtered, they were all combined into one database for regression analysis. Summary statistics for the combined database are presented in Supplementary Table S1. It is noted that due to sporadic instrument outages and differing start times, the number of 15-minute data points collected on the vines of each variety were different. Also, units for R_c and D_c in the final regressions were converted to kW/m^2 and kPa respectively to avoid problematically small coefficients that resulted when using the units specified for Equations 1 and 2.

Data compilation, filtering, and graphing were performed in the *R* software environment (R Core Team, 2021) using several functions from the *dplyr* package (Wickham *et al.*, 2021b) and the *ggplot2* package (Wickham *et al.*, 2021a).

2. Bulk stomatal conductance

As presented by Gowdy *et al.* (2022) bulk stomatal conductance (g_{bs}) is determined from the 2-layer energy flux model for sparse crop canopies, like those of vineyards, as developed by Shuttleworth and Wallace (1985) using a Penman-Monteith (PM) type equation for calculation of latent heat flux from the vine canopy as given by Equation 1 (Lhomme *et al.*, 2012).

▸ Equation 1: $\lambda E_c = \frac{\Delta R_c + \rho Cp(D_c)/r_{bh}}{\Delta + \gamma\left(n + \frac{r_{bs}}{r_{bh}}\right)}$ (W m^{-2})

This equation is first rearranged to give the bulk stomatal resistance (r_{bs}) as given in Equation 2 and followed by g_{bs} from Equation 3.

▸ Equation 2:

$$r_{bs} = \frac{\Delta R_c * r_{bh} + \rho C p D_c}{\lambda E_c \gamma} - r_{bh}\left(\frac{\Delta}{\gamma} - n\right) \qquad (\text{s m}^{-1})$$

and bulk stomatal conductance is given by inversion:

▸ Equation 3: $g_{bs} = r_{bs}^{-1}$ (m s^{-1})

where:

E_c = transpiration flux from canopy per unit ground area (g m^{-2} s^{-1})

λ = latent heat of vaporization for water = 2257 (J g^{-1})

D_c = vapour pressure deficit at mean canopy height (Pa)

R_c = net radiation absorbed by the vine canopy per unit ground area (W m^{-2})

r_{bs} = bulk stomatal resistance (s m^{-1})

r_{bh} = bulk boundary layer resistance to heat flux (s m^{-1})

n = 2 for grapevine leaves with stomata on one side only

γ = psychrometric constant at 1 atm and 20°C = 65.8 (Pa C°$^{-1}$)

Δ = rate of change in saturation vapour pressure versus temperature = 145 (Pa C°$^{-1}$)

ρCp = heat content per unit volume of air at 20°C = 1212 (Pa C°$^{-1}$)

The output units for Equation 2 (s m^{-1}) and Equation 3 (m s^{-1}) result when the above input units are used, with all conductance/resistance and fluxes expressed in terms of unit area of vineyard ground attributable to each vine (i.e., row spacing x vine spacing).

The method of Riou *et al.* (1989) was used for estimating the amount of such radiation absorbed by grapevine canopy (R_c) as needed for input to Equations 1 or 2. Relying on inputs of canopy dimensions, row spacing, vine spacing, and canopy porosity, along with measured solar radiation and various solar angles, this model outputs radiation flux (W m^{-2}) of shortwave radiation absorbed by the vine canopy expressed in terms of the unit area of vineyard ground attributable to each vine (i.e., row spacing x vine spacing) (Riou *et al.,* 1989).

The canopy bulk boundary layer resistance to heat flux (r_{bh}) needed as input to Equations 1 and 2 is given by Equation 4 below and represents the canopy-level summation of the leaf-level boundary layer resistances across all leaves in the canopy stated in terms of unit ground area (Lhomme *et al.,* 2012):

▸ Equation 4: $r_{bh} = \frac{r_{bl}}{2 * LAI}$ (s m^{-1})

where:

r_{bl} = leaf-level boundary layer resistance (s m^{-1}) = 25 s m^{-1} per Shuttleworth and Wallace (1985).

LAI = leaf area index.

Using input data from the compiled and filtered database, g_{bs} was calculated using Equations 2 and 3 and r_{bh} was calculated using Equation 4, with the results of both appended back to the database.

3. Response variable transformation

Biological and environmental data often demonstrate non-linear relationships and collinearity between variables (Dormann *et al.*, 2013), which must be addressed in order to meet the required assumptions of ordinary least squared regression analysis.

Figure 1 presents bulk stomatal conductance (g_{bs}) plotted versus 15-minute canopy vapour pressure deficit (D_c), net radiation absorbed by the canopy (R_c), and interpolated predawn leaf water potential (Ψ_{PD}) for each variety separately. In previous studies of *Vitis vinifera* varieties, non-linear relationships between g_{bs} and D_c have been observed (Prieto *et al.*, 2010; Lu *et al.*, 2003). A similar non-linear relationship also existed between the g_{bs} and Ψ_{PD} data, while the relationship between g_{bs} and R_c did not demonstrate any non-linear characteristics.

To address the non-linearity in the relationship between g_{bs} and both D_c and Ψ_{PD}, a $\log_{10}$ transformation of g_{bs} was used as the response variable in subsequent regression analyses. For the data from all 10 vines combined, Figure 2 presents the $\log_{10}$ transformation of g_{bs} plotted against 15-minute D_c, R_c, and interpolated Ψ_{PD} data demonstrating roughly linear relationships for each relationship. The effect of the data filters can also be seen in the plot panels for R_c and D_c in both Figures 1 and 2.

4. Predictor variable selection

The process of selecting variables to consider for inclusion in the regression analysis began with Ψ_{PD} and the key input variables to Equations 2 and 3 for calculation of g_{bs}, including R_c, D_c, and r_{bh}.

Vine water status, as measured by Ψ_{PD}, is well understood to have an effect on conductance, and was found to have a statistically significant and strong effect on g_{bs} in the final regression analysis. But unlike the 15-minute interval measurements of R_c and D_c, the periodic measurements of Ψ_{PD} will miss some of the range and response of the varying water status experienced by the vines. This is unavoidable due to the nature of measuring leaf water potential. The final regression analysis also shows R_c and D_c as having statistically significant and strong effects on g_{bs} and were retained in the final model.

Regression model iterations including r_{bh} as a predictor generated statistically significant ($p < 0.05$) coefficients for that variable, but they explained only a small portion of variation in g_{bs}. This also concurs with findings from Gowdy *et al.* (2022) and from Shuttleworth and Wallace (1985) that found r_{bh} to be of much less importance than the other input variables in the determination of g_{bs}. Furthermore, there was strong collinearity between r_{bh} and Ψ_{PD}, which contributed to very high variance inflation factors for the two variables and their interactions.

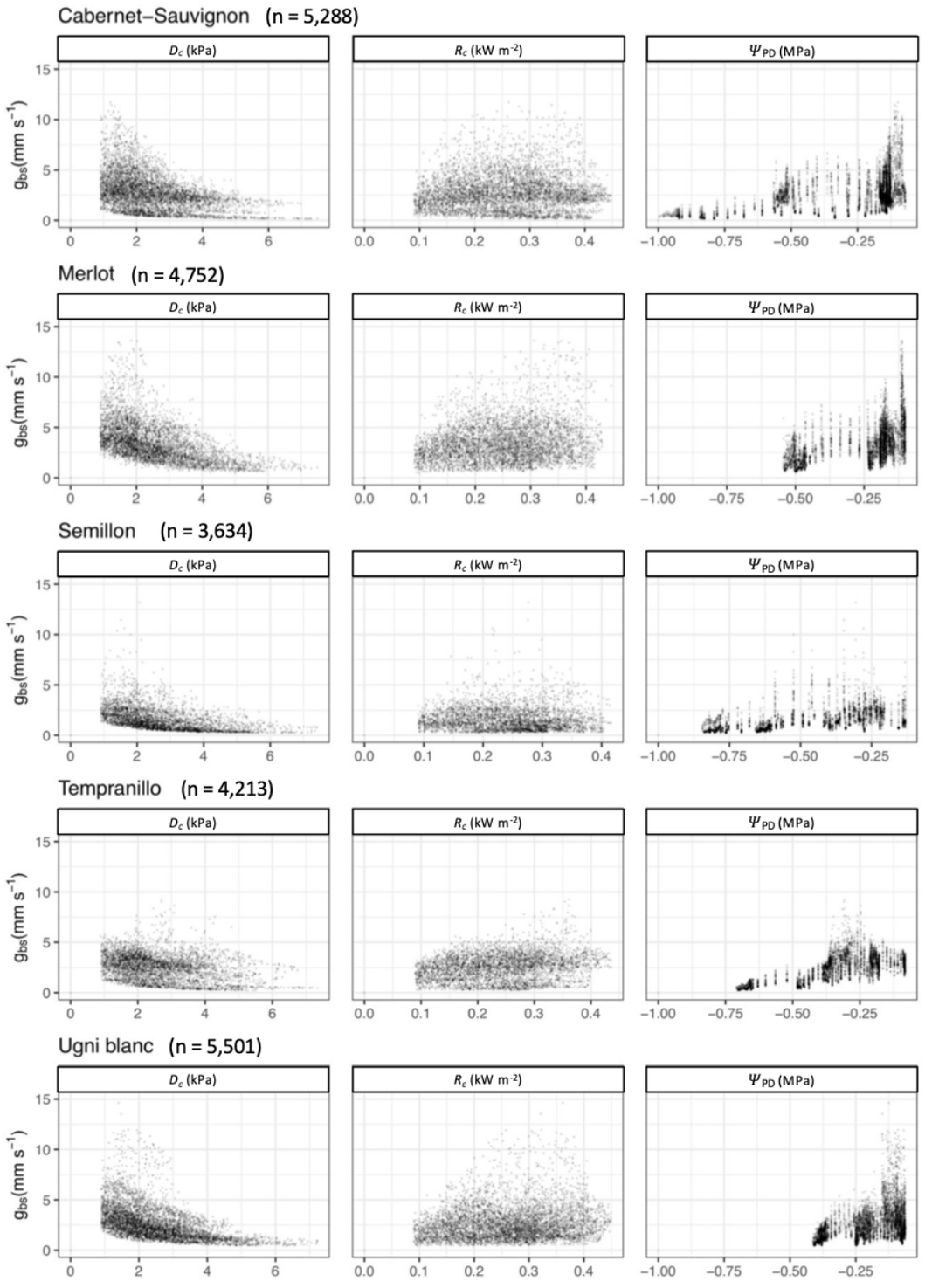

FIGURE 1. Bulk stomatal conductance (g_{bs}) plotted versus canopy vapour pressure deficit (D_c), net radiation absorbed by the canopy (R_c), and interpolated predawn leaf water potential (Ψ_{PD}) by variety.

This collinearity is associated with the leaf loss that coincides with the gradual increase in water stress over the season and the resulting more negative Ψ_{PD}.

As a result, r_{bh} was excluded from the final regression analysis. E_c is also an input to Equation 2, but was not considered in the regressions as regulation of g_{bs} is how plants control E_c, making the two strongly collinear and of minimal explanatory value.

In addition to the main effects of the predictor variables described above, interaction terms between these variables were also considered in a regression analysis based on standardized data (Supplementary Table S2). While nearly all interaction terms from this regression had coefficients that

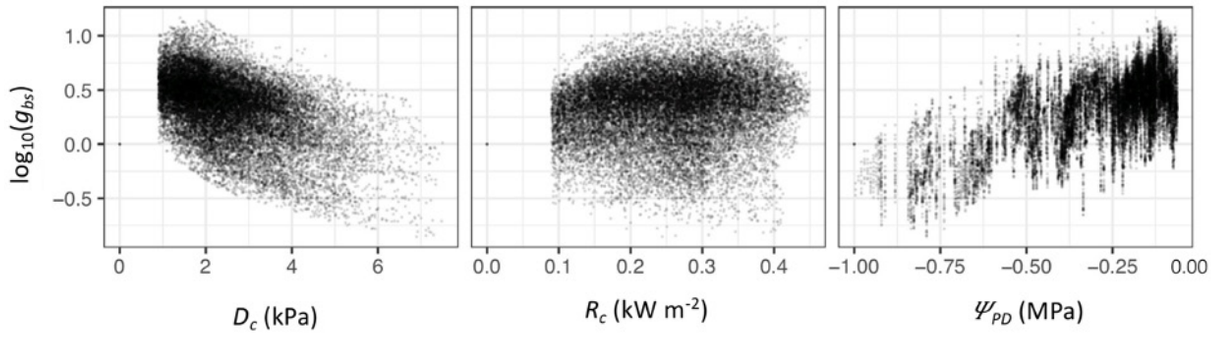

FIGURE 2. Log_{10} transformation of g_{bs} plotted versus canopy vapour pressure deficit (D_c), net radiation absorbed by the canopy (R_c), and interpolated predawn leaf water potential (Ψ_{PD}) with data from all 10 vines together (n = 23388).

were significant ($p < 0.05$), their importance was not great compared to those for the main effects and furthermore, added considerable complexity to the model and its interpretability. The regression analysis was run again on the standardized data with the interaction terms excluded, which resulted in a model fit that was only slightly diminished and much simpler to interpret (Supplementary Table S3). For reference, the same regression without interactions was run again with raw data (Supplementary Table S4). The predictor variables retained in the final multiple linear regression model, therefore, were R_c, D_c and Ψ_{PD}, with no interaction terms included.

5. Multiple linear regression and ad hoc analysis

The formula used for the regression analysis of $log_{10}(g_{bs})$ as the response variable with R_c, D_c, and Ψ_{PD} as continuous predictor variables and *variety* as a grouping factor variable is given by Equation 5:

▸ Equation 5: $log_{10}(g_{bs}) \sim (R_c + D_c + \Psi_{PD}) * variety$

Expressed in equation form, the multiple linear regression model resulting for each variety using the predictors selected above is given by Equation 6:

▸ Equation 6: $g_{bs} = \beta_0 + \beta_{Rc} * R_c + \beta_{Dc} * D_c + \beta_\psi * \Psi_{PD}$

where:

β_0 = y-axis intercept

$\beta_{Rc} = R_c$ regression coefficient

$\beta_{Dc} = D_c$ regression coefficient

$\beta_\psi = \Psi_{PD}$ regression coefficient.

The effect of each predictor is characterized by the associated coefficient (β), which when based on raw data represents the average change in the response variable for a given unit change in each of the predictor variables. The regression analysis was also performed using standardized response and predictor variable data, whereby each data point is both subtracted by the mean and divided by the standard deviation of all values for a given variable. In this way the data is both centered on zero and has the same scale in terms of standard deviations from the mean. When based on standardized data, the resulting coefficients for the predictors represent the mean change in the response variable for one standard deviation change in the associated predictor. This is useful because with all data on the same scale, the absolute value of the regression coefficients for the different predictors can be compared directly to understand their relative effect on the response variable (Frost, 2020).

Due to sporadic instrument outages and differing start times, the number of 15-minute data points collected on the vines of each variety were different. Also, even though it was minimized by the filtering and transformations, there was still a low level of collinearity between input variables as observed in the variance inflation factors (described further below). Such factors may complicate an ad hoc comparison of regression coefficients that might be obtained from regressions performed using the data from each variety separately.

As an alternative, the filtered and transformed data from all vines was pooled together and a factor variable representing the different varieties was added, which is then included as part of an interaction term with each of the predictors. From this regression, the coefficients for each predictor are calculated as *marginal mean slopes*, whereby the average effect of each predictor on the response variable is calculated separately for each variety, at the same time assuming the mean values of all the other predictor variables (Searle *et al.*, 1980; Lenth *et al.*, 2022). This approach is useful in that the p-value for each interaction term indicates the significance of the difference between the coefficients (Lenth *et al.*, 2022). The regression coefficients of the selected predictor variables were all significant ($p < 0.05$) and explained meaningful amounts of the variation in $log_{10}(g_{bs})$. For comparison purposes, separate variety specific regressions were performed (not presented) which gave identical regression coefficients and nearly identical intercept terms, suggesting that, in fact, the effect of the unbalanced data between varieties and the interactions were not that great.

After each iteration, variance inflation factors (VIFs) were evaluated for each predictor variable and its interactions, if included. VIFs identify the presence and strength of interactions between model terms. The goal is for the VIFs for each predictor variable and any interaction

term to be below a generally accepted value of 5.0, with 1.0 representing complete independence (Frost, 2020). The VIFs for predictors R_c, D_c, and Ψ_{PD} in the final regression model based on combined data, whether standardized, or raw were 1.2, 1.2, and 1.1 respectively, which are well below a standard threshold of 5.0. The low VIFs suggest the effects of interactions were either successfully avoided by variable selection, or removed by filtering and transformation. The coefficient of determination (r^2), or the fraction of $log_{10}(g_{bs})$ variance explained by the final model, whether based on raw or standardized data, was 0.701. Both the adjusted r^2 and predicted r^2 were also 0.701 in both cases, suggesting the model is not overfitted.

For multiple linear regression it is also important to check whether the underlying ordinary least square assumptions are satisfied. In Supplementary Figures S1 a) and b) the standardized model residuals are normally distributed with a mean of zero. Supplementary Figure S1 c) shows relatively constant variance in the standardized residuals plotted versus fitted values (i.e., no heteroscedasticity) and in Supplementary Figures S1 d) through f) there is relatively constant variance in the standardized residuals plotted versus the three predictor variable plots (i.e., no endogeneity). The residual plots for regressions based on standardized and raw data were identical, except for being on different scales.

Multiple linear regression analysis was performed in the *R* software environment (R Core Team, 2021) using the *lm* function; variance inflation factors were calculated using the *vif* function of the *car* package (Fox *et al.*, 2021); and calculation of estimated marginal means of linear slopes were done using the *emtrends* function from the *emmeans* package (Lenth *et al.*, 2022).

6. Transpiration simulations

The variety-specific predictor variable coefficients from the regression analysis based on raw data were used to simulate and compare vine canopy transpiration across varieties and to compare against simulations from an existing vineyard water balance model.

6.1 Water balance model simulations

A time series of daily vine canopy transpiration and associated soil water depletions were estimated using the vineyard water balance model developed by Pieri and Bois (2007), as based on the methodology described in Lebon *et al.* (2003). For the purpose of comparison with regression model-based simulations, actual data from the 2020 growing season was also used in the water balance model, consisting of measured daily maximum and minimum temperature, rainfall, and solar radiation. It also requires inputs of canopy configuration and porosity and assumptions regarding total transpirable soil water (*TTSW*). This model, however, is not parameterized to distinguish differences in transpiration response between varieties, so only one generic transpiration estimate is produced.

The vine canopy transpiration component of evapotranspiration in this model is determined by first calculating the fraction of total incident radiation to the vineyard that is captured by the canopy (minus that which is reflected) using the method of Riou *et al.* (1989). This fraction is then applied to the reference crop evapotranspiration (i.e., soil evaporation plus vine transpiration) as calculated by the Penman equation and adjusted early in the season to account for gradual development of the canopy starting at budbreak. Also accounting for soil evaporation and precipitation, the model then tracks the daily balance of water in the assumed volume of *TTSW* within the vineyard root zone.

As the fraction of remaining total available transpirable soil water (*FTSW*) in the root zone decreases, the model factors in reductions in transpiration to account for the reduced stomatal conductance associated with increasing drought stress. This reduction is achieved by a function relating the ratio of modeled vine transpiration to maximum vine transpiration (TV/TV_{max}) versus *FTSW* as presented in Pieri and Gaudillere (2005).

6.2 Regression model-based simulations

Using the final variety-specific regression equations, transpiration was simulated by first calculating a time series of $log_{10}(g_{bs})$ for each variety using a common 15-minute time series of predictor input data as measured during the 2020 growing season. For this purpose, the predictor coefficients determined based on raw data were used. A time series of g_{bs} was then calculated by taking the base 10 antilog of $log_{10}(g_{bs})$, which was then input to Equation 1 along with the corresponding R_c, D_c, and r_{bh} data to give an associated estimate of transpiration summed on a daily basis (mm day^{-1}). All data, including that which was filtered before the regression analysis, was included in the transpiration simulations.

For these simulations, a time series of 15-minute measurements of R_c, and D_c from the 2020 season was selected from a representative vine. The time series of R_c and D_c across all 10 vines measured in the study were very similar. This is understandable as the amount of radiation absorbed by the vine canopy (R_c) is strongly influenced by canopy dimensions and porosity (Riou *et al.*, 1989; Pieri, 2010), which were all very similar for each vine. And while vapour pressure deficit in the vine canopy (D_c) was affected by vine transpiration, it was more strongly driven by ambient vapour pressure deficits and hence fairly similar across vines. Therefore, for the purpose of a common input to the transpiration simulations, R_c and D_c data from the vine with the most complete time series over the season was used in the regression equations for each of the five varieties.

The regression model-based simulations also require an input of Ψ_{PD}. For this purpose, a daily time series of Ψ_{PD} was developed using the output of *FTSW* from the corresponding water balance model, which was converted to Ψ_{PD} by the *FTSW* to Ψ_{PD} relationships published in Figure 3 of Lebon *et al.,* 2003. Differing levels of *TTSW* were assumed in the water balance model in order to understand the effect of the differing levels of associated *FTSW* on the regression

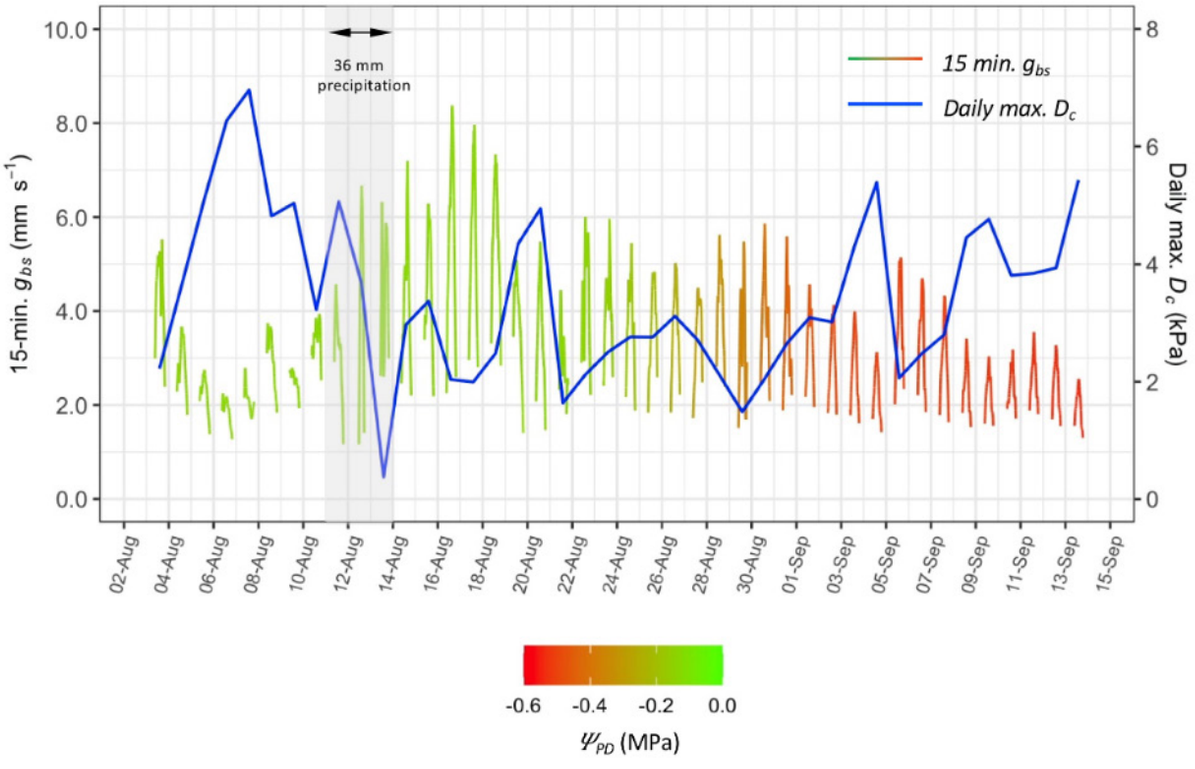

FIGURE 3. 15-minute time series of calculated bulk stomatal conductance (g_{bs}, mm s^{-1}) and daily maximum D_c (kPa) between 3 August through 13 September 2020 from one vine of Cabernet-Sauvignon, with colour gradient representing corresponding Ψ_{PD} (MPa).

model-based simulations. *TTSW* values of 240 mm and 200 mm were selected as described further below.

RESULTS

1. Bulk stomatal conductance (g_{bs})

Figure 3 presents the 15-minute time series of bulk stomatal conductance (g_{bs}, mm s^{-1}) calculated with Equations 2 and 3 using, as an example, data between 3 August through 13 September 2020 from one vine of Cabernet-Sauvignon. Gaps in this time series are due to filtering of data early in the morning and late in the evening that otherwise caused erratic determinations of g_{bs}. This line also has a colour gradient representing the corresponding interpolated Ψ_{PD}. Studies using somewhat similar approaches to estimate vine canopy conductance based on whole-plant transpiration measurements in vineyards found similar overall conductance levels and responses to changes in micrometeorological variables for c.v. Merlot (Zhang *et al.*, 2012), c.v. Sultana (Lu *et al.*, 2003), and cv. Thompson Seedless (Bai *et al.*, 2015), although the latter two studies did not evaluate the effect of decreasing soil water content over the season.

A noticeable increase in overall levels of conductance is observed after 36 mm of precipitation on 11 through 13 August, the only significant rainfall of the study period. Predawn water potential measurements have been found to equilibrate with portions of the root zone having the highest water content (Améglio *et al.*, 1999), such as may occur near the surface after a rainfall. A gradual decrease in both the overall level and diurnal amplitude of g_{bs} is also observed in conjunction with the gradual onset of more negative Ψ_{PD} (i.e., water deficit stress) and/or perhaps developmental changes over the season. It also appears that the g_{bs} timeseries is rather negatively correlated with the D_c timeseries (blue line in Figure 3) as might be expected from previous studies (Prieto *et al.*, 2010; Lu *et al.*, 2003).

The time series of g_{bs} calculated in this way for each vine, along with the corresponding predictor variable data time series were used in the subsequent multiple linear regressions.

2. Predictor variable coefficients

The multiple linear regression of $log_{10}(g_{bs})$ as the response variable with R_c, D_c, and Ψ_{PD} as continuous predictor variables was performed using *variety* as a grouping factor variable as described in Equation 5. From this, the regression coefficients (β) for the predictor variables as described in Equation 6 are presented separately for each variety in Tables 1a through 1c for R_c, D_c, and Ψ_{PD} respectively. As these coefficients were developed based on standardized data, the magnitudes of their absolute values are directly comparable across varieties.

There appears to be more of a differentiation between varieties in the Ψ_{PD} coefficients in Table 1c when compared to the predictors. And while the R_c coefficient covers a similar relative range, three of the varieties have very similar values in the mid-range as seen in Table 1a.

Table 2a presents the same predictor coefficients as in Tables 1a through 1c, instead listed in rows by variety, together with the y-axis intercepts. Based on standardized data,

TABLE 1. Predictor variable coefficients (β) from regressions using standardized $log_{10}(g_{bs})$ as the response and standardized predictors R_c (a), D_c (b), and Ψ_{PD} (c) as continuous predictor variables, by variety with upper and lower 95 % confidence limits (CL), p-values, and compact letter display of pairwise significance.

	Variety	β	Low CL	Upper CL	p-value	Pairwise
a) Standardized R_c coefficient	Cabernet-Sauvignon	0.161	0.145	0.177	~ 0	a
	Semillon	0.225	0.202	0.247	~ 0	b
	Tempranillo	0.255	0.235	0.275	~ 0	b
	Ugni blanc	0.256	0.241	0.272	~ 0	b
	Merlot	0.303	0.285	0.320	~ 0	c
b) Standardized D_c coefficient	Ugni blanc	-0.625	-0.641	-0.609	~ 0	a
	Semillon	-0.582	-0.601	-0.563	~ 0	b
	Cabernet-Sauvignon	-0.560	-0.577	-0.543	~ 0	b
	Merlot	-0.558	-0.575	-0.541	~ 0	b
	Tempranillo	-0.433	-0.452	-0.414	~ 0	c
c) Standardized Ψ_{PD} coefficient	Merlot	0.423	0.400	0.445	~ 0	a
	Semillon	0.458	0.441	0.474	~ 0	ab
	Ugni blanc	0.485	0.458	0.512	~ 0	bc
	Cabernet-Sauvignon	0.512	0.499	0.524	~ 0	c
	Tempranillo	0.773	0.752	0.794	~ 0	d

Pairwise comparisons with shared letters not significantly different ($p < 0.05$).

TABLE 2. Regression coefficients (β) from final regression analysis for y-axis intercepts and predictor variables R_c, D_c, and Ψ_{PD} with a) standardized data, and b) raw data.

	Variety	β_0	β_{Rc}	β_{Dc}	β_{Ψ}
a) with standardized data	Merlot	-0.036	0.303	-0.558	0.423
	Semillon	-0.036	0.225	-0.582	0.458
	Ugni blanc	-0.036	0.256	-0.625	0.485
	Cabernet-Sauvignon	-0.036	0.161	-0.560	0.512
	Tempranillo	-0.036	0.255	-0.433	0.773
b) with raw data	Merlot	0.788	1.110	-0.146	0.066
	Semillon	0.788	0.824	-0.153	0.072
	Ugni blanc	0.788	0.940	-0.164	0.076
	Cabernet-Sauvignon	0.788	0.589	-0.147	0.080
	Tempranillo	0.788	0.934	-0.114	0.121

the magnitude of the absolute value of these coefficients are now comparable across the three predictors for a given variety.

It is observed the absolute value of the D_c and Ψ_{PD} coefficients are comparable in magnitude, with both being about 1.5 to 3.5 times larger than the R_c coefficient, suggesting their greater importance in explaining the variation of g_{bs} observed in each corresponding variety. The relatively subdued response to R_c may be due to the relative consistent range of R_c measurements. As it is driven by solar radiation, whose daily fluctuations change only gradually over the season, R_c does not have the larger extremes seen in D_c and Ψ_{PD}, which then elicit greater responses from the vines.

For reference, Table 2b presents the same predictor coefficients based on raw data. When based on raw data, these coefficients can be used to calculate modeled bulk stomatal conductance ($\hat{g}_{bs}$) in its original units (mm s^{-1}) as needed for subsequent sensitivity analysis and transpiration simulations.

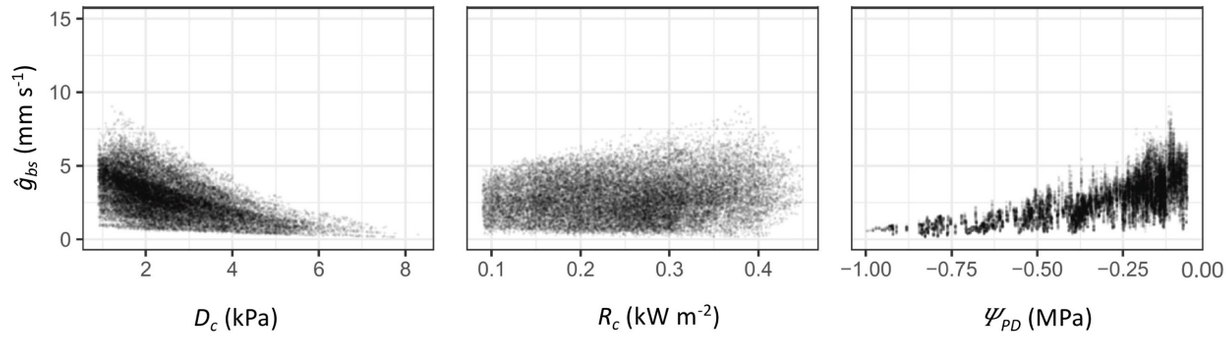

FIGURE 4. Back-transformed $\hat{g}_{bs}$ from modeled $log_{10}(g_{bs})$ plotted against D_c, R_c, and Ψ_{PD} data used for regressions from all 10 vines combined.

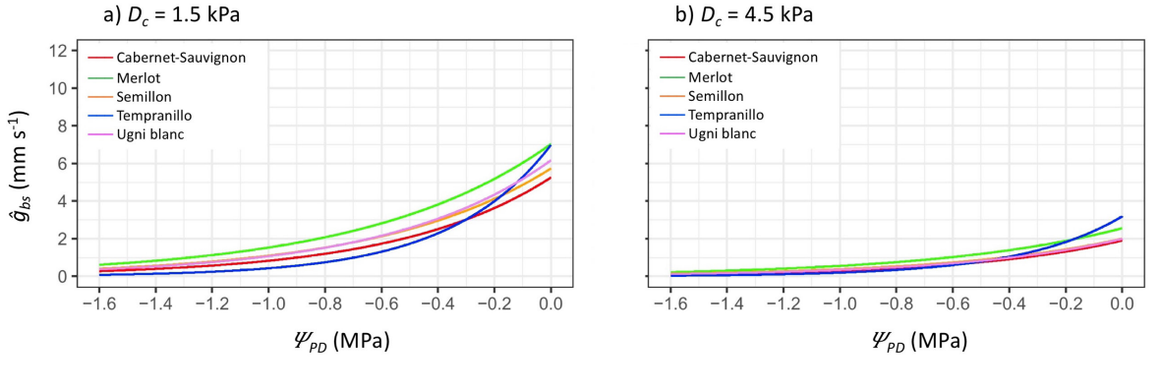

FIGURE 5. Modeled g_{bs} ($\hat{g}_{bs,}$ mm s^{-1}) by variety plotted against a hypothetical range of Ψ_{PD} (MPa) with mean value of R_c = 0.263 kW m^{-2} and: a) D_c = 1.5 kPa; and b) D_c = 4.5 kPa.

The intercepts (β_0) in each of Tables 2a and 2b are the same across all varieties due to the regression model being performed on data from all varieties combined. If the regression is performed between $log_{10}(g_{bs})$ and R_c, D_c, and Ψ_{PD} without including the variety factor variable, the intercept of the regression is zero, as expected when using standardized data. Including the factor variable for variety, however, introduces a very small intercept term (-0.036) as seen in Table 2a.

3. Sensitivity analysis

The modeled bulk stomatal conductance ($\hat{g}_{bs}$), as back transformed from modeled $log_{10}(g_{bs})$, and then plotted against R_c, D_c, and Ψ_{PD} shows the non-linear relationships with D_c and Ψ_{PD} that remains after regression (Figure 4). The range of $\hat{g}_{bs}$ is somewhat diminished compared to the plots of raw calculated g_{bs} presented in Figure 1 due to the least squared fitting of the regression model.

Plots of $\hat{g}_{bs}$ across a range of hypothetical Ψ_{PD} values at fixed levels of D_c = 1.5 kPa and D_c = 4.5 kPa, and with a mean value of R_c = 0.263 kW m^{-2} (Figure 5) show higher overall $\hat{g}_{bs}$, and a greater spread in $\hat{g}_{bs}$ between varieties at lower D_c and more positive Ψ_{PD} levels. And in keeping with its larger Ψ_{PD} coefficient in Table 1c, $\hat{g}_{bs}$ for Tempranillo drops more quickly when compared to the other varieties as Ψ_{PD} becomes more negative. The general effect of increasing D_c can also be observed on the overall decrease in the $\hat{g}_{bs}$ response curve with respect to Ψ_{PD}.

In keeping with the lower absolute value of its D_c coefficient in Table 1b, the $\hat{g}_{bs}$ of Tempranillo drops off less quickly than the other varieties as D_c increases (Figure 6).

Again, with a mean value of R_c = 0.263 kW m^{-2}, the effect of more negative Ψ_{PD} = - 0.5 MPa versus Ψ_{PD} = - 0.1 MPa can also be observed in Figure 6, with an overall decrease in the levels of $\hat{g}_{bs}$ at the more negative Ψ_{PD}. The spread between varieties, however, remains fairly similar between the two levels of Ψ_{PD}, particularly at lower levels of D_c.

The biggest differences in $\hat{g}_{bs}$ between varieties were observed in the plot of $\hat{g}_{bs}$ versus R_c, particularly at the lower D_c = 1.5 kPa (Figure 7, panel a). The steeper nature of the $\hat{g}_{bs}$ versus R_c curve for Merlot is also particularly noticeable at D_c = 1.5 kPa, corresponding with its larger R_c coefficient when compared to other varieties as presented in Table 1a. Also, due to the smaller absolute value for its D_c coefficient observed above in Table 1b and Figure 6, the $\hat{g}_{bs}$ for Tempranillo does not decrease as much relative to the other varieties at higher D_c = 4.5 kPa (Figure 7, panel b). A fixed value of Ψ_{PD} = -0.1 MPa was assumed in both panels of Figure 7. However, the R_c coefficients are generally smaller than those for the other predictors, as can be seen in the relative flatness of the lines in Figure 7, and won't have as strong an influence on $\hat{g}_{bs}$.

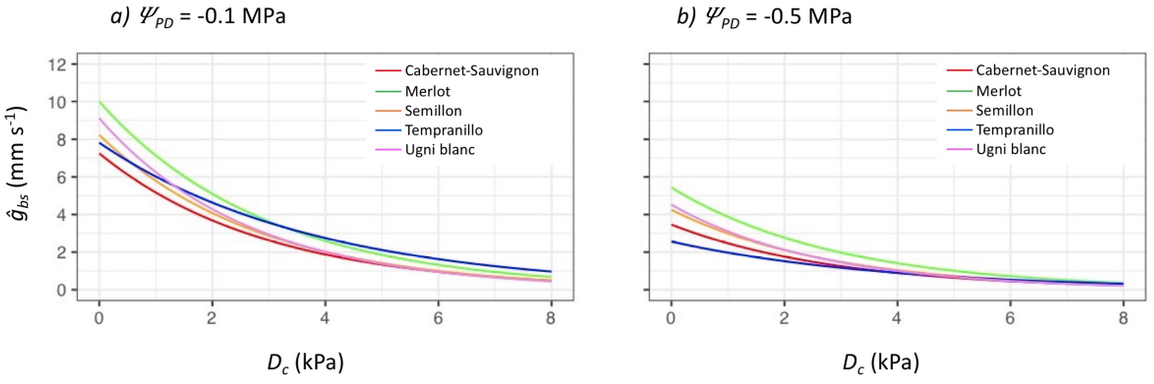

FIGURE 6. Modeled g_{bs} ($\hat{g}_{bs,}$ mm s^{-1}) by variety plotted against a hypothetical range of D_c (kPa) with mean value of R_c = 0.263 kW m^{-2} and: a) Ψ_{PD} = -0.1 MPa; and b) Ψ_{PD} = -0.5 MPa.

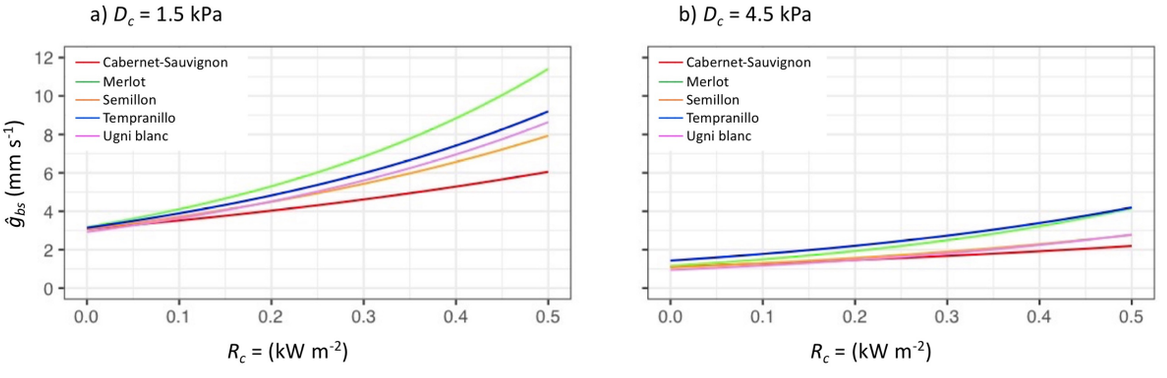

FIGURE 7. Modeled g_{bs} ($\hat{g}_{bs,}$ mm s^{-1}) by variety plotted against a hypothetical range of R_c (kW m^{-2}) with Ψ_{PD} = -0.1 MPa and : a) D_c = 1.5 kPa; and b) D_c = 4.5 kPa.

In general, across all the plots in Figures 5 through 7, Merlot has the highest $\hat{g}_{bs}$, while either Tempranillo, or Cabernet-Sauvignon had the lowest.

4. Simulations of canopy transpiration

Similar to the differences in $\hat{g}_{bs}$ observed in the sensitivity analysis above, the simulated transpiration for the five varieties calculated using their respective regression equations found Merlot to have the greatest daily and season total simulated transpiration, while Tempranillo or Cabernet-Sauvignon had the lowest, regardless of the *TTSW* assumption (coloured lines in Figure 8a for TTSW = 240 mm and Figure 8b for TTSW = 200). It is also observed that the ordering in the relative rates of simulated transpiration by variety in both figures follows the same ordering in magnitude of the Ψ_{PD} regression coefficients by variety in Table 1c. Although there are greater differences between varieties for the R_c coefficient as seen in Table 1a, the overall magnitude of the R_c coefficients relative to those for D_c and Ψ_{PD} were substantially smaller and hence have less effect on $\hat{g}_{bs}$.

These simulations were based on common R_c and D_c input data from the 2020 season, with the time series of Ψ_{PD} needed for the simulations generated by the water balance model using climate data for the same time period and assuming *TTSW* = 240 mm (Figure 8, panel a) and *TTSW* = 200 mm (Figure 8, panel b). An estimate of *TTSW* for the vineyard was not available, so these were considered two values within a reasonable range, which resulted in simulated transpiration rates similar to those measured during the study. The median daily transpiration rate from 30 June to 15 September 2020 period ranged, depending on the vine, between 1.0 to 2.7 mm per day, with the maximum ranging between 2.5 and 5.5 mm/day, depending on the vine. As they are all based on the same input data time series, these regression model-based simulations provide another form of sensitivity analysis across varieties, this time in terms of transpiration.

Comparison of the regression model-based simulation of vine transpiration (Figures 8a and 8b, coloured lines) against the water balance model simulation of vine transpiration excluding soil evaporation (Figures 8a and 8b, black line) finds generally good agreement. It appears, however, that the water balance model tends towards relatively higher transpiration, and therefore faster reductions in *FTSW* early in the season, leading to stronger transpiration reductions and underestimation of transpiration later in the season.

In the water balance model, transpiration is regulated as a function of *FTSW* using the relative transpiration (TV/TV_{max}) versus *FTSW* function from Pieri and Gaudillere (2005).

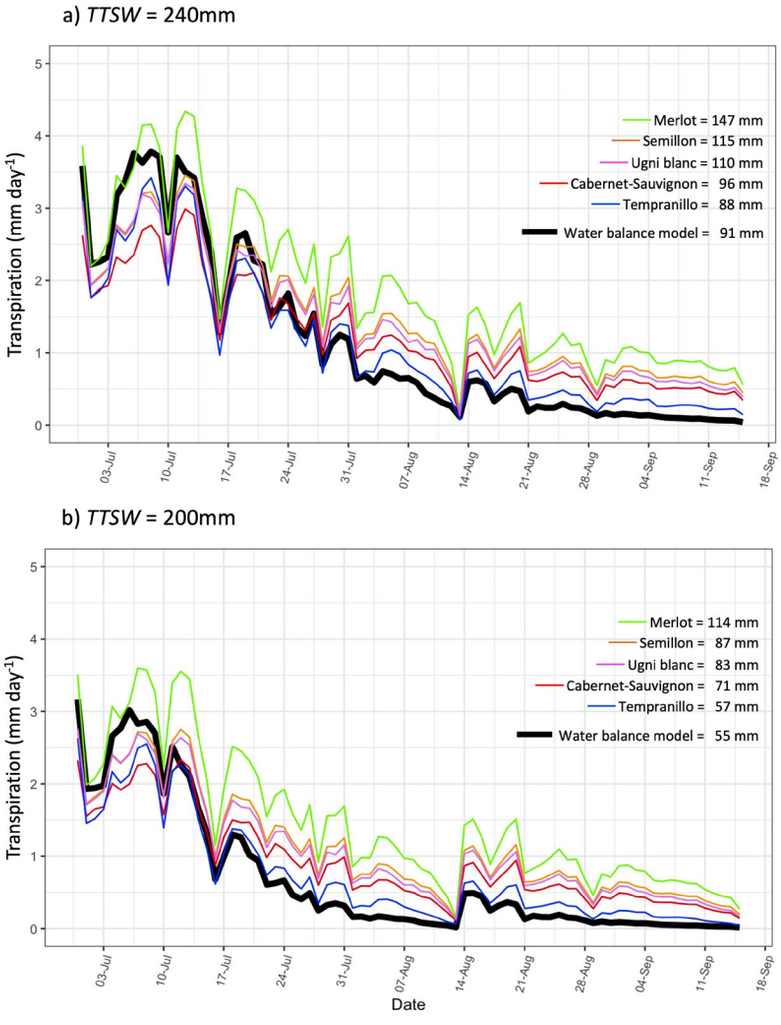

FIGURE 8. Daily total vine transpiration (mm/day) for five varieties simulated using regression coefficients (coloured lines) and the daily total vine transpiration (mm/day) component from the water balance (black line) in panel a) based on *TTSW* = 240mm and in panel b) based *TTSW* = 200mm, with legend including total simulated transpiration from 30 June to 15 September 2020.

Relative transpiration (TV/TV_{max}) is the ratio of simulated transpiration at a given moment over its maximum.

Figure 9 presents a plot of the (TV/TV_{max}) versus *FTSW* function used to regulate transpiration in the water balance model (black line) together with plots of the relative transpiration (TV/TV_{max}) versus *FTSW* resulting from the regression model-based simulations (coloured lines). From Figure 9 it appears that at higher *FTSW*, as experienced earlier in the season, the relative transpiration function of the water balance model allows for relatively higher transpiration compared to that resulting from the regression models. This may explain the relatively higher daily transpiration simulated by the water balance model as observed early in the season in Figure 8, leading to a more rapid reduction in *FTSW*, and hence reduced transpiration by way of the relative transpiration versus *FTSW* reduction function later in the season.

The ordering of the TV/TV_{max} versus *FTSW* curves resulting from the regression model-based simulations (coloured lines in Figure 9) are also the same as for the Ψ_{PD} coefficients in Table 1c. The variety most affected by *FTSW* in Figure 9 is also Tempranillo, as suggested by it having the largest Ψ_{PD} coefficient in Table 1c, remembering in all cases, that *FTSW* and Ψ_{PD} are assumed to follow the relationship published in Figure 3 of Lebon *et al.,* 2003.

As the *TTSW* assumption in water balance modeling decreases, for example from 240 mm to 200 mm as depicted in Figures 8 a) and b), the resulting overall *FTSW* also decreases. By way of the transpiration reduction functions in Figure 9 this leads to relatively lower rates of simulated daily transpiration seen in Figure 8 b) for *TTSW* = 200 mm, when compared to Figure 8 a) for *TTSW* = 240 mm. It should be noted, however, there is a great deal of uncertainty regarding the *TTSW* assumption in the water balance modeling due to soil conditions, planting density, and the rooting characteristics of different scion/rootstock combinations and even individual vines. Regardless, water balance model runs based on reasonable *TTSW* assumptions are still useful for comparison purposes.

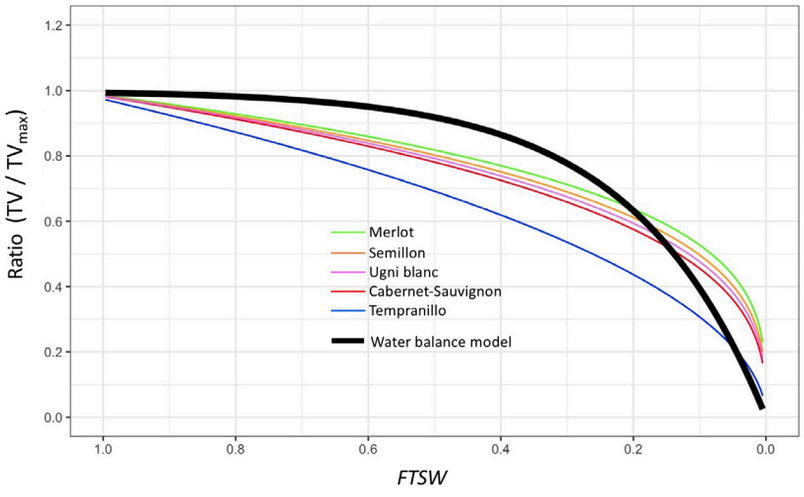

FIGURE 9. Relative transpiration (transpiration / maximum transpiration) as calculated using the regression models versus *FTSW* for each variety (coloured lines) and the transpiration reduction function used in the water balance model (black line).

Based on a constructed time series of input data, the simulation results above are not intended for direct comparisons to measured data, although there is general agreement with the latter falling in a similar range. In order to fully model transpiration using the variety specific regression equations, they would need to be part of a model that tracks soil water deficits or associated Ψ_{PD} over the course of the season in a feedback loop to the transpiration calculation. With differing transpiration rates for each variety, the resulting time series of *FTSW*, and hence Ψ_{PD} over the season, and its subsequent effect on transpiration would each be different.

DISCUSSION

In this study we developed estimates of whole-vine bulk stomatal conductance (g_{bs}) and quantified its response to changes in the environment. Vapour pressure deficit in the vine canopy (D_c) and available soil water, as measured by predawn leaf water potential (Ψ_{PD}) were the main drivers of changes in g_{bs}, with net radiation absorbed by the vine canopy (R_c) also being a factor. Although environmental drivers predominated, some significant differences in modeled g_{bs} ($\hat{g}_{bs}$) response, and hence simulated water use over the growing season were observed between varieties, however, further study may be needed to better distinguish those differences.

For both *TTSW* assumptions presented in Figures 8, Merlot had the highest seasonal total simulated transpiration, followed in order by Semillon, Ugni blanc, Cabernet-Sauvignon, and Tempranillo. As the inputs of R_c, D_c and Ψ_{PD} to the calculation of simulated transpiration are the same for all varieties, these differences are then explained by overall differences in $\hat{g}_{bs}$. Beginning after the week of 17 July the ordering of varieties in terms of daily transpiration are the same as for the seasonal totals. Prior to then, however, the ordering is somewhat different, particularly with regards to Tempranillo, which demonstrated a lesser decrease in $\hat{g}_{bs}$ in response to increasing D_c (Figure 6) and greater decrease in $\hat{g}_{bs}$ in response to decreasing Ψ_{PD} (Figure 7) when compared to the other four varieties. This suggests Tempranillo puts greater emphasis on responding to decreasing Ψ_{PD} than on increasing D_c when compared to the other varieties.

Field studies of Tempranillo found similar dynamics with regard to leaf-level stomatal conductance in response to predawn water potential (Medrano *et al.*, 2003; Yuste *et al.*, 2004; Intrigliolo and Castel, 2006), although they did not evaluate the effects of vapour pressure deficit on conductance, nor compare against any of the of the other varieties included in this study.

The change in the steepness of the slope in the relationship between $\hat{g}_{bs}$ versus R_c, D_c or Ψ_{PD} is observed in Figures 5, 6, and 7 respectively to be generally greater, whether positive or negative, for those varieties with higher $\hat{g}_{bs}$ at non-limited conditions. It is possible that varieties with higher overall g_{bs} under less limited conditions will transpire more, deplete soil water reserves more quickly, and experience greater levels of soil water stress (or require more irrigation) sooner in the season than those with overall lower g_{bs}. As Ψ_{PD} becomes more negative, then varieties with a greater β_Ψ will begin to restrict their transpiration more quickly to adapt. The rooting depth and resulting *TTSW* for individual vines or varieties are also an important consideration in the onset of soil water depletion.

The different ways varieties regulate their conductance may result from varying interplay between the different physiological mechanisms controlling stomata. For example, studies on typically anisohydric varieties Merlot (Zhang *et al.* 2012) and Semillon (Rogiers *et al.*, 2012) observed anisohydric response at higher soil water status, but more isohydric response for both varieties at low soil water status. In both cases, the isohydric response followed a general tendency towards greater stomatal closure in response to increasing vapour pressure deficit, with this greater response

positively correlated with the reference gas exchange rate at non-limiting conditions, as expected from empirical and theoretical modeling (Oren *et al.*, 1999; Domec and Johnson, 2012). In the Merlot study, it was suggested the transition from anisohydric to isohydric response was due to a decrease in whole-plant conductance associated with decreased soil water status (Zhang *et al.* 2012). The Semillon study suggested the shift to isohydric behavior was attributable to increased abscisic acid (ABA) generated at lower soil water status, which further increases stomatal sensitivity to VPD (Rogiers *et al.* 2012). ABA produced in vine roots was also linked to changes in stomatal sensitivity in Cabernet-Sauvignon (Speirs *et al.*, 2013; Tramontini *et al.*, 2014). Changes in nature of the stomatal response for several varieties were also observed as a function of water deficit by Levin *et al.* (2020) with Tempranillo being slightly more sensitive to changes in Ψ_{PD} than Cabernet-Sauvignon.

Direct comparison of varietal responses from different studies is confounded by differences in measurement methodology, such as leaf-level measurement of conductance by gas exchange versus canopy conductance by sap flow. Future comparisons using the same, or similar methods would lead to more comparable results. And while all vines measured in this study were subjected to the same climate conditions, the g_{bs} response would be better characterized if using data from different years with different relative amounts of R_c, D_c and Ψ_{PD}. The results could also likely be different if performed in an overall different climate (*e.g.*, southern Europe, or northern France). Even being performed in the same vineyard, the soil conditions around the root zone of individual vines and its effect on rooting volume, access to water, etc., however, can still be quite heterogeneous (Smart *et al.*, 2006). Therefore, with only two vines per variety included in this study, the results could potentially be biased by the specific growing conditions experienced by those vines. Rootstocks and canopy management could also be influencing factor on vine conductance (Marguerit *et al.,* 2012; Picón-Toro *et al.*, 2012) and should be taken into consideration.

CONCLUSIONS

Based on data collected in a vineyard setting, a multiple linear regression analysis was able to quantify relationships across five different grapevine varieties between vine canopy bulk stomatal conductance (g_{bs}) and three key environmental variables: net radiation absorbed by the vine canopy (R_c); vapour pressure deficit in the vine canopy (D_c); and predawn lewaf water potential (Ψ_{PD}). Depending on the variety, D_c and Ψ_{PD} each had about 1.5 to 3.5 times greater effect on g_{bs} than R_c. Of these two more important predictors, the Ψ_{PD} regression coefficient was more differentiated across the five varieties than was the D_c coefficient. And while there was a significant range in R_c coefficients across varieties, their overall lower values mean they had less of an influence on the differences in g_{bs} response across varieties compared to the other predictors.

A comparison of transpiration simulated using the above regression results found a significant difference in the total growing season transpiration between varieties that appeared to be driven in large part by the difference across varieties in the effect of Ψ_{PD} on g_{bs}. There was a general tendency towards greater modeled g_{bs} ($\hat{g}_{bs}$) response, whether positive or negative, to changes in the predictor variables when $\hat{g}_{bs}$ at non-limiting conditions was greater. It was also observed that Tempranillo puts greater emphasis on reducing its g_{bs} in response to decreasing Ψ_{PD} than in response to increasing D_c when compared to the other varieties. These transpiration simulations were also compared against those from an accepted vineyard water balance model and found similar results, although there appeared to be differences between the two approaches in the rate at which conductance, and hence transpiration is reduced as a function of decreasing soil water content (i.e., increasing water deficit stress).

The input data needed for this type of study naturally contains non-linearity and collinearity, but careful selection of variables, transformations and filtering made for a readily interpretable multiple linear regression model that satisfied ordinary least squares assumptions. And aside from providing a method for quantifying the response of vine conductance to different environmental variables, the described approach may provide a basis for variety-specific modeling of the vine transpiration component in vineyard water balance models. Knowledge of such differences in g_{bs} response could help with selection of varieties that are better suited for future changes in certain growing conditions in a region, such as the prevailing atmospheric vapour pressure deficits, or amount of precipitation and expected soil water depletions.

ACKNOWLEDGEMENTS

The authors would like to thank Guillermo Gutiérrez, Eylul Kadaifci, and Alfonso Domínguez Zamudio for their very hard work in the vineyard, and to the INRAE, UEVB, F-33882, Villenave d'Ornon, France, for its management of the VitAdapt vineyard and assistance with implementing instrumentation.

This study has been carried out with financial support from Jas. Hennessy & Co. (16100 Cognac, France) and the French National Research Agency (ANR) in the frame of the Investments for the future Programme, within the Cluster of Excellence COTE (ANR-10-LABX-45). The VitAdapt vineyard is supported by the Conseil Interprofessionnel des Vins de Bordeaux (CIVB), the Conseil Régional d'Aquitaine, Bordeaux University through LabEx and the Institut National de Recherche pour l'Agriculture, l'Alimentation et l'Environnement (INRAE).

REFERENCES

Allen, R. G., Pereira, L. S., Raes, D., & Smith, M. (1998). FAO Irrigation and drainage paper No. 56. *Rome: Food and Agriculture Organization of the United Nations*, *56*, 97–156.

Améglio, T., Archer, P., Cohen, M., Valancogne, C., Daudet, F., Dayau, S., & Cruiziat, P. (1999). Significance and limits in the use of predawn leaf water potential for tree irrigation. *Plant and Soil*, *207*(2), 155–167. https://doi.org/10.1023/A:1026415302759

Bai, Y., Zhu, G., Su, Y., Zhang, K., Han, T., Ma, J., Wang, W., Ma, T., & Feng, L. (2015). Hysteresis loops between canopy conductance of grapevines and meteorological variables in an oasis ecosystem. *Agricultural and Forest Meteorology*, *214–215*, 319–327. https://doi.org/10.1016/j.agrformet.2015.08.267

Chahine, A., Dupont, S., Sinfort, C., & Brunet, Y. (2014). Wind-Flow Dynamics Over a Vineyard. *Boundary-Layer Meteorology*, *151*(3), 557–577. https://doi.org/10.1007/s10546-013-9900-4

Charrier, G., Delzon, S., Domec, J. C., Zhang, L., Delmas, C. E., Merlin, I., Corso, D., King, A., Ojeda, H., Ollat, N., Prieto, J., Scholash, T., Skinner, P., van Leeuwen, C., & Gambetta, G. A. (2018). Drought will not leave your glass empty: Low risk of hydraulic failure revealed by long-term drought observations in world's top wine regions. *Science Advances*, *4*(1), eaao6969. https://doi.org/10.1126/sciadv.aao6969

Chaves, M. M., Zarrouk, O., Francisco, R., Costa, J. M., Santos, T., Regalado, A. P., Rodrigues, M. L., & Lopes, C. M. (2010). Grapevine under deficit irrigation: Hints from physiological and molecular data. *Annals of Botany*, *105*(5), 661–676. https://doi.org/10.1093/aob/mcq030

Choné, X., van Leeuwen, C., Dubourdieu, D., & Gaudillère, J. P. (2001). Stem Water Potential is a Sensitive Indicator of Grapevine Water Status. *Annals of Botany*, *87*(4), 477–483. https://doi.org/10.1006/anbo.2000.1361

Costa, J. M., Ortuño, M. F., Lopes, C. M., Chaves, M. M., Costa, J. M., Ortuño, M. F., Lopes, C. M., & Chaves, M. M. (2012). Grapevine varieties exhibiting differences in stomatal response to water deficit. *Functional Plant Biology*, *39*(3), 179–189. https://doi.org/10.1071/FP11156

Destrac-Irvine, A., & van Leeuwen, C. (2017). The Vitadapt project: Extensive phenotyping of a wide range of varieties in order to optimize the use of genetic diversity within the *Vitis vinifera* species as a tool for adaptation to a changing environment. *Proceedings of Climwine 2016 - Sustainable Grape and Wine Production in the Context of Climate Change.*, 165–171.

Domec, J.-C., & Johnson, D. M. (2012). Does homeostasis or disturbance of homeostasis in minimum leaf water potential explain the isohydric versus anisohydric behavior of *Vitis vinifera* L. cultivars? *Tree Physiology*, *32*(3), 245–248. https://doi.org/10.1093/treephys/tps013

Dormann, C. F., Elith, J., Bacher, S., Buchmann, C., Carl, G., Carré, G., Marquéz, J. R. G., Gruber, B., Lafourcade, B., Leitão, P. J., Münkemüller, T., McClean, C., Osborne, P. E., Reineking, B., Schröder, B., Skidmore, A. K., Zurell, D., & Lautenbach, S. (2013). Collinearity: A review of methods to deal with it and a simulation study evaluating their performance. *Ecography*, *36*(1), 27–46. https://doi.org/10.1111/j.1600-0587.2012.07348.x

Fox, J., Weisberg, S., Price, B., Adler, D., Bates, D., Baud-Bovy, G., Bolker, B., Ellison, S., Firth, D., Friendly, M., Gorjanc, G., Graves, S., Heiberger, R., Krivitsky, P., Laboissiere, R., Maechler, M., Monette, G., Murdoch, D., Nilsson, H., … R-Core. (2021). *car: Companion to Applied Regression* (3.0-12) [Computer software]. https://CRAN.R-project.org/package=car

Franks, P. J., Drake, P. L., & Froend, R. H. (2007). Anisohydric but isohydrodynamic: Seasonally constant plant water potential gradient explained by a stomatal control mechanism incorporating variable plant hydraulic conductance. *Plant, Cell & Environment*, *30*(1), 19–30. https://doi.org/10.1111/j.1365-3040.2006.01600.x

Frost, J. (2020). *Regression Analysis: An Intuitive Guide for Using and Interpreting Linear Models*. Statistics By Jim Publishing.

Gowdy, M., Pieri, P., Suter, B., Marguerit, E., Destrac-Irvine, A., Gambetta, G., & van Leeuwen, C. (2022). Estimating Bulk Stomatal Conductance in Grapevine Canopies. *Frontiers in Plant Science*, *13*. https://www.frontiersin.org/article/10.3389/fpls.2022.839378

Herrera, J. C., Calderan, A., Gambetta, G. A., Peterlunger, E., Forneck, A., Sivilotti, P., Cochard, H., & Hochberg, U. (2021). Stomatal responses in grapevine become increasingly more tolerant to low water potentials throughout the growing season. *The Plant Journal: For Cell and Molecular Biology*. https://doi.org/10.1111/tpj.15591

Hochberg, U., Rockwell, F. E., Holbrook, N. M., & Cochard, H. (2018). Iso/Anisohydry: A Plant–Environment Interaction Rather Than a Simple Hydraulic Trait. *Trends in Plant Science*, *23*(2), 112–120. https://doi.org/10.1016/j.tplants.2017.11.002

Intrigliolo, D. S., & Castel, J. R. (2006). Vine and soil-based measures of water status in Tempranillo vineyard. *Vitis*, *45*(4), 157–163. https://doi.org/10.5073/vitis.2006.45.157-163

Keller, M. (2015). *The Science of Grapevines: Anatomy and Physiology* (2nd edition). Academic Press.

Kelliher, F. M., Leuning, R., Raupach, M. R., & Schulze, E.-D. (1995). Maximum conductances for evaporation from global vegetation types. *Agricultural and Forest Meteorology*, *73*(1), 1–16. https://doi.org/10.1016/0168-1923(94)02178-M

Krounbi, L., & Lazarovitch, N. (2011). Soil Hydraulic Properties Affecting Root Water Uptake. In J. Gliński, J. Horabik, and J. Lipiec (Eds.), *Encyclopedia of Agrophysics* (pp. 748–754). Springer Netherlands. https://doi.org/10.1007/978-90-481-3585-1_149

Lavoie-Lamoureux, A., Sacco, D., Risse, P.-A., & Lovisolo, C. (2017). Factors influencing stomatal conductance in response to water availability in grapevine: A meta-analysis. *Physiologia Plantarum*, *159*(4), 468–482. https://doi.org/10.1111/ppl.12530

Lebon, E., Dumas, V., Pieri, P., & Schultz, H. R. (2003). Modelling the seasonal dynamics of the soil water balance of vineyards. *Functional Plant Biology*, *30*(6), 699–710. https://doi.org/10.1071/FP02222

Lenth, R. V., Buerkner, P., Herve, M., Love, J., Miguez, F., Riebl, H., & Singmann, H. (2022). *emmeans: Estimated Marginal Means, aka Least-Squares Means* (1.7.2) [Computer software]. https://CRAN.R-project.org/package=emmeans

Levin, A. D., Williams, L. E., & Matthews, M. A. (2020). A continuum of stomatal responses to water deficits among 17 wine grape cultivars (*Vitis vinifera*). *Functional Plant Biology*, *47*(1), 11–25. https://doi.org/10.1071/FP19073

Lhomme, J. P., Montes, C., Jacob, F., & Prévot, L. (2012). Evaporation from Heterogeneous and Sparse Canopies: On the Formulations Related to Multi-Source Representations. *Boundary-Layer Meteorology*, *144*(2), 243–262. https://doi.org/10.1007/s10546-012-9713-x

Lovisolo, C., Perrone, I., Carra, A., Ferrandino, A., Flexas, J., Medrano, H., & Schubert, A. (2010). Drought-induced changes in development and function of grapevine (*Vitis* spp.) organs and in their hydraulic and non-hydraulic interactions at the whole-plant level: A physiological and molecular update. *Functional Plant Biology*, *37*(2), 98. https://doi.org/10.1071/FP09191

Lu, P., Yunusa, I. A. M., Walker, R. R., & Müller, W. J. (2003). Regulation of canopy conductance and transpiration and their modelling in irrigated grapevines. *Functional Plant Biology*, *30*(6), 689–698. https://doi.org/10.1071/FP02181

Marguerit, E., Brendel, O., Lebon, E., van Leeuwen, C., & Ollat, N. (2012). Rootstock control of scion transpiration and its acclimation to water deficit are controlled by different genes. *New Phytologist*, *194*(2), 416–429. https://doi.org/10.1111/j.1469-8137.2012.04059.x

Martínez-Vilalta, J., Poyatos, R., Aguadé, D., Retana, J., & Mencuccini, M. (2014). A new look at water transport regulation in plants. *New Phytologist*, *204*(1), 105–115. https://doi.org/10.1111/nph.12912

McElrone, A. J., Choat, B., Gambetta, G. A., & Brodersen, C. R. (2013). Water uptake and transport in vascular plants. *Nature Education Knowledge*, *4*(6). http://www.nature.com.zhongjivip.net/scitable/knowledge/library/water-uptake-and-transport-in-vascular-plants-103016037

Medrano, H., Escalona, J. M., Cifre, J., Bota, J., & Flexas, J. (2003). A ten-year study on the physiology of two Spanish grapevine cultivars under field conditions: Effects of water availability from leaf photosynthesis to grape yield and quality. *Functional Plant Biology*, *30*(6), 607–619. https://doi.org/10.1071/fp02110

Mendoza, V., Pazos, M., Garduño, R., & Mendoza, B. (2021). Thermodynamics of climate change between cloud cover, atmospheric temperature and humidity. *Scientific Reports*, *11*(1), 21244. https://doi.org/10.1038/s41598-021-00555-5

Monteith, J., & Unsworth, M. (2013). *Principles of Environmental Physics: Plants, Animals, and the Atmosphere*. Academic Press.

Oren, R., Sperry, J. S., Katul, G. G., Pataki, D. E., Ewers, B. E., Phillips, N., & Schäfer, K. V. R. (1999). Survey and synthesis of intra- and interspecific variation in stomatal sensitivity to vapour pressure deficit. *Plant, Cell & Environment*, *22*(12), 1515–1526. https://doi.org/10.1046/j.1365-3040.1999.00513.x

Pellegrino, A., Gozé, E., Lebon, E., & Wery, J. (2006). A model-based diagnosis tool to evaluate the water stress experienced by grapevine in field sites. *European Journal of Agronomy*, *25*(1), 49–59. https://doi.org/10.1016/j.eja.2006.03.003

Picón-Toro, J., González-Dugo, V., Uriarte, D., Mancha, L. A., & Testi, L. (2012). Effects of canopy size and water stress over the crop coefficient of a "Tempranillo" vineyard in south-western Spain. *Irrigation Science*, *30*(5), 419–432. https://doi.org/10.1007/s00271-012-0351-3

Pieri, P. (2010). Modelling radiative balance in a row-crop canopy: Row–soil surface net radiation partition. *Ecological Modelling*, *221*(5), 791–801. https://doi.org/10.1016/j.ecolmodel.2009.11.019

Pieri, P., & Bois, B. (2007). *Feuille de calcul excel du modèle de bilan hydrique de la vigne* (1 beta) [Computer software].

Pieri, P., & Gaudillere, J. P. (2005). Vines water stress derived from a soil water balance model—Sensitivity to soil and training system parameters. *XIV International GiESCO Viticulture Congress, Geisenheim, Germany, 23-27 August, 2005*, 457–463. https://www.cabdirect.org/cabdirect/abstract/20053214000

Prieto, J. A., Lebon, É., & Ojeda, H. (2010). Stomatal behavior of different grapevine cultivars in response to soil water status and air water vapour pressure deficit. *OENO One*, *44*(1), 9–20. https://doi.org/10.20870/oeno-one.2010.44.1.1459

Pou, A., Medrano, H., Tomàs, M., Martorell, S., Ribas-Carbó, M., & Flexas, J. (2012). Anisohydric behaviour in grapevines results in better performance under moderate water stress and recovery than isohydric behaviour. *Plant and Soil*, *359*(1), 335–349. https://doi.org/10.1007/s11104-012-1206-7

R Core Team. (2021). *R: A Language and Environment for Statistical Computing*. R Foundation for Statistical Computing. https://www.R-project.org/

Riou, C., Valancogne, C., & Pieri, P. (1989). Un modèle simple d'interception du rayonnement solaire par la vigne—Vérification expérimentale. *Agronomie*, *9*(5), 441–450. https://doi.org/10.1051/agro:19890502

Rogiers, S. Y., Greer, D. H., Hatfield, J. M., Hutton, R. J., Clarke, S. J., Hutchinson, P. A., & Somers, A. (2012). Stomatal response of an anisohydric grapevine cultivar to evaporative demand, available soil moisture and abscisic acid. *Tree Physiology*, *32*(3), 249–261. https://doi.org/10.1093/treephys/tpr131

Sack, L., & Holbrook, N. M. (2006). Leaf Hydraulics. *Annual Review of Plant Biology*, *57*(1), 361–381. https://doi.org/10.1146/annurev.arplant.56.032604.144141

Scholander, P. F., Bradstreet, E. D., Hemmingsen, E. A., & Hammel, H. T. (1965). Sap Pressure in Vascular Plants. *Science*. https://doi.org/10.1126/science.148.3668.339

Schultz, H. R. (1996). Water relations and photosynthetic responses of two grapevine cultivars of different geographical origin during water stress. *Acta Horticulturae*, *427*, 251–266. https://doi.org/10.17660/ActaHortic.1996.427.30

Schultz, H. R. (2003). Differences in hydraulic architecture account for near-isohydric and anisohydric behaviour of two field-grown *Vitis vinifera* L. cultivars during drought. *Plant, Cell & Environment*, *26*(8), 1393–1405. https://doi.org/10.1046/j.1365-3040.2003.01064.x

Searle, S. R., Speed, F. M., & Milliken, G. A. (1980). Population Marginal Means in the Linear Model: An Alternative to Least Squares Means. *The American Statistician*, *34*(4), 216–221. https://doi.org/10.1080/00031305.1980.10483031

Shimazaki, K., Doi, M., Assmann, S. M., & Kinoshita, T. (2007). Light Regulation of Stomatal Movement. *Annual Review of Plant Biology*, *58*(1), 219–247. https://doi.org/10.1146/annurev.arplant.57.032905.105434

Shmueli, G. (2010). *To Explain or To Predict?* (SSRN Scholarly Paper ID 1351252). Social Science Research Network. https://doi.org/10.2139/ssrn.1351252

Shuttleworth, W. J., & Wallace, J. S. (1985). Evaporation from sparse crops-an energy combination theory. *Quarterly Journal of the Royal Meteorological Society*, *111*(469), 839–855. https://doi.org/10.1002/qj.49711146910

Smart, D. R., Breazeale, A., & Zufferey, V. (2006). Physiological Changes in Plant Hydraulics Induced by Partial Root Removal of Irrigated Grapevine (*Vitis vinifera* cv. Syrah). *American Journal of Enology and Viticulture*, *57*(2), 201–209.

Smart, R., & Robinson, M. (1991). *Sunlight Into Wine*. WINETITLES.

Speirs, J., Binney, A., Collins, M., Edwards, E., & Loveys, B. (2013). Expression of ABA synthesis and metabolism genes under different irrigation strategies and atmospheric VPDs is associated with stomatal conductance in grapevine (*Vitis vinifera* L. cv Cabernet-Sauvignon). *Journal of Experimental Botany*, *64*(7), 1907–1916. https://doi.org/10.1093/jxb/ert052

Sperry, J. S., Saliendra, N. Z., Pockman, W. T., Cochard, H., Cruiziat, P., Davis, S. D., Ewers, F. W., & Tyree, M. T. (1996). New evidence for large negative xylem pressures and their measurement by the pressure chamber method. *Plant, Cell & Environment*, *19*(4), 427–436. https://doi.org/10.1111/j.1365-3040.1996.tb00334.x

Tardieu, F., & Simonneau, T. (1998). Variability among species of stomatal control under fluctuating soil water status and evaporative demand: Modelling isohydric and anisohydric behaviours. *Journal of Experimental Botany*, *49*(90001), 419–432. https://doi.org/10.1093/jexbot/49.suppl_1.419

Tramontini, S., van Leeuwen, C., Domec, J.-C., Destrac-Irvine, A., Basteau, C., Vitali, M., Mosbach-Schulz, O., & Lovisolo, C. (2012). Impact of soil texture and water availability on the hydraulic control of plant and grape-berry development. *Plant and Soil*, *368*(1–2), 215–230. https://doi.org/10.1007/s11104-012-1507-x

Tramontini, S., Döring, J., Vitali, M., Ferrandino, A., Stoll, M., & Lovisolo, C. (2014). Soil water-holding capacity mediates hydraulic and hormonal signals of near-isohydric and near-anisohydric Vitis cultivars in potted grapevines. *Functional Plant Biology*, *41*(11), 1119. https://doi.org/10.1071/FP13263

van Leeuwen, C., Destrac-Irvine, A., Dubernet, M., Duchêne, E., Gowdy, M., Marguerit, E., Pieri, P., Parker, A., de Rességuier, L.,

& Ollat, N. (2019a). An Update on the Impact of Climate Change in Viticulture and Potential Adaptations. *Agronomy*, *9*(9), 514. https://doi.org/10.3390/agronomy9090514

van Leeuwen, C., Pieri, P., Gowdy, M., Ollat, N., & Roby, J.-P. (2019b). Reduced density is an environmental friendly and cost effective solution to increase resilience to drought in vineyards in a context of climate change: *OENO One*, *53*(2), 129–146. https://doi.org/10.20870/oeno-one.2019.53.2.2420

Wickham, H., Chang, W., Henry, L., Pedersen, T. L., Takahashi, K., Wilke, C., Woo, K., Yutani, H., Dunnington, D., & RStudio. (2021a). *ggplot2: Create Elegant Data Visualisations Using the Grammar of Graphics* (3.3.5) [Computer software]. https://CRAN.R-project.org/package=ggplot2

Wickham, H., François, R., Henry, L., Müller, K., & RStudio. (2021b). *dplyr: A Grammar of Data Manipulation* (1.0.7) [Computer software]. https://CRAN.R-project.org/package=dplyr

Wild, M. (2009). Global dimming and brightening: A review. *Journal of Geophysical Research: Atmospheres*, *114*(D10). https://doi.org/10.1029/2008JD011470

Willett, K. M., Dunn, R. J. H., Thorne, P. W., Bell, S., de Podesta, M., Parker, D. E., Jones, P. D., & Williams Jr., C. N. (2014). HadISDH land surface multi-variable humidity and temperature record for climate monitoring. *Climate of the Past*, *10*(6), 1983–2006. https://doi.org/10.5194/cp-10-1983-2014

Yuste, J., Rubio, J. A., & Péez, A. (2004). Influence of Plant Density and Water Regime on Soil Water Use, Water Relations and Productivity of Trellis-Trained Tempranillo Grapevines. *Acta Horticulturae*, *646*, 187–193. https://doi.org/10.17660/ActaHortic.2004.646.24

Zhang, Y., Oren, R., & Kang, S. (2012). Spatiotemporal variation of crown-scale stomatal conductance in an arid *Vitis vinifera* L. cv. Merlot vineyard: Direct effects of hydraulic properties and indirect effects of canopy leaf area. *Tree Physiology*, *32*(3), 262–279. https://doi.org/10.1093/treephys/tpr120

Zufferey, V., Cochard, H., Ameglio, T., Spring, J.-L., & Viret, O. (2011). Diurnal cycles of embolism formation and repair in petioles of grapevine (*Vitis vinifera* cv. Chasselas). *Journal of Experimental Botany*, *62*(11), 3885–3894. https://doi.org/10.1093/jxb/err081.